 

***OPTICAL GATES***

https://doi.org/10.1070/QEL16279

# All-optical XNOR gate based on 2D photonic-crystal ring resonators

Tamer A. Moniem

***Abstract.*** **A novel all-optical XNOR gate is proposed, which combines the nonlinear Kerr effect with photonic-crystal ring resonators (PCRRs). The total size of the proposed optical XNOR gate based on photonic crystals with a square lattice of silicon rods is equal to 35×21 μm. The proposed structure has a bandgap in the range from 0.32 to 0.44. To confirm the operation and feasibility of the overall system use is made of analytical and numerical simulation using the dimensional finite difference time domain (FDTD) and plane wave expansion (PWE) methods.**

***Keywords:*** *photonic crystals, photonic-crystal ring resonators, optical gates, optical switches.*

## 1. Introduction

In recent years all-optical logic gates [1–6] and optical logic devices based on photonic crystal (PC) structures have been reported, including an optical demultiplexer [7, 8], optical encoder [9, 10], optical decoders [11–13] and optical flip flops [14–16]. These optical devices play a crucial role in implementing all-optical communication systems and optical signal processing networks. So far so many works have been devoted to the development of all-optical logic gates based on PC structures, where photonic crystals are the most promising due to their high transmission efficiency, high quality factor and stability.

This paper proposes a novel structure for implementing an all-optical XNOR gate based on two photonic-crystal ring resonators (PCRRs). The fundamental structure used for designing the proposed XNOR gate is a square lattice of Si rods immersed in air. This optical logic device is very interesting and important for integrated optics, since it can be used to implement a set of optical combination logic circuits in 2D photonic crystals such as a half adder, full adder, logic comparator and parity check circuit in optical communication systems.

## 2. Photonic-crystal ring resonator

A photonic-crystal ring resonator (PCRR) is fabricated in the fundamental structure by removing some rods as shown in Fig. 1 [11, 17], where a 9×9 array of dielectric rods is removed for producing a resonance at a wavelength of 1550 nm. This optical PCRR made of a square lattice array of Si rods with a refractive index of 3.39 in air measures 18×15 μm. The radius of rods is $r = 0.21a$, where $a = 630$ nm is the lattice constant of the structure.

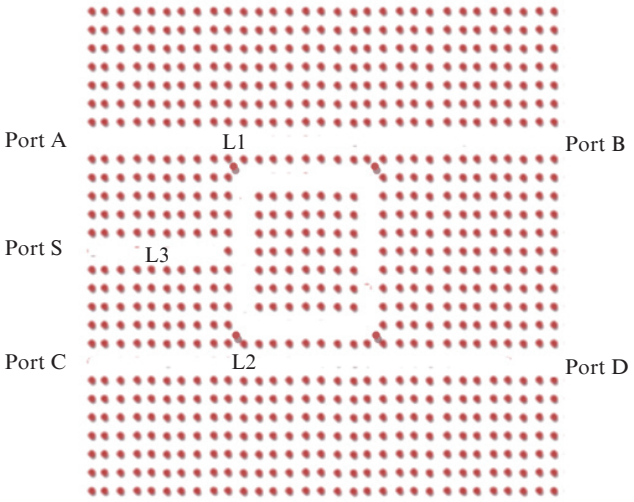


**Figure 1.** Schematic structure of the photonic-crystal ring resonator.

The PCRR structure is formed by three waveguides (L1, L2, L3), four ports (A, B, C, D) and a control port (S). The optical structure is excited through the input port A with an optical bias signal at a wavelength $\lambda = 1550$ nm. Depending on the control signal coupled into port S, the bias signal exits from one of output ports (B, C, D).

When the signal of the control port S is equal to 0 (0 mW), the input bias optical signal from port A at a resonance wavelength $\lambda = 1550$ nm is dropped through waveguide L1 into the ring and flows to port C by coupling to the drop waveguide L2 (Fig. 2a). When the optical signal of the control port S = 1 (100 mW) is coupled to the PCRR, the field intensity in the ring resonator increases, thereby preventing the coupling of the bias input signal from port A to the ring and coupling it to port B (Fig. 2b), where the higher intensity of the light results in changes in the effective refractive index of the ring based on the Kerr nonlinear effect. Hence, the resonance wavelength is shifted and consequently no drop occurs for the high intensity light with a 1550 nm wavelength.

**Tamer A. Moniem** Misr University for Science & Technology, Al-Motamayez District, P.O. Box 77, 6th of October City, Cairo, Egypt; e-mail: tamerkhawaga@yahoo.com, tamer.abdelmoniem@must.edu.eg

Received 19 December 2016; revision received 22 January 2017
*Kvantovaya Elektronika* **47** (2) 169–172 (2017)
Submitted in English

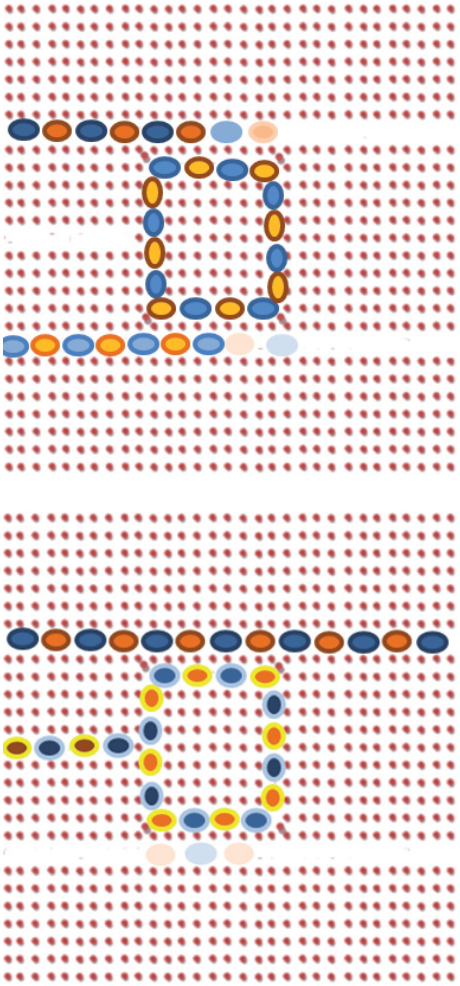


**Figure 2.** (Colour online) Optical field pattern distribution in the PCRR for S = (a) 0 and (b) 1.

## 3. Theoretical method and design of an all-optical XNOR gate

The exclusive NOR (XNOR) gate is a digital logic gate whose function is the logical complement of the exclusive OR (XOR) gate [18]. A high output (1) results if both of the inputs to the gate are the same; otherwise, if one but not both inputs are high (1), a low output (0) results (see Table 1).

The paper presents an all-optical XNOR gate based on a square lattice of 2D PCs with a size of 35×21 μm (Fig. 3). The distance between two neighbouring rods is equal to $a$ = 630 nm, and the radius of the rod is $r = 0.21a$. The proposed optical XNOR gate is composed of two photonic crystal ring resonators (PCRR1, PCRR2) with radius of $5a$, and two waveguides (L1, L2). The inputs A and B of XNOR are coupled into the ring resonators PCRR1 and PCRR2, respectively. The optical XNOR gate is triggered by the input optical bias signal at the left end of waveguide L1, while the output signal (Y) of XNOR is obtained at the right end of waveguide L1. In the corners of all PCRRs and waveguide L2, there are extra rods shifted towards the corner by $0.707a$ with the same refractive index and rod radius to eliminate the backscattering at the corners [10, 13, 15]. To prevents the vertical propagation of the light, the semiconductor rods in air are supported by a low-refractive index material ($SiN_x$, $SiO_x$, polymers) [19–21].

**Table 1.** Truth table of the XNOR gate.

| Inputs | | Output |
|---|---|---|
| A | B | Y = A XNOR B |
| 0 | 0 | 1 |
| 0 | 1 | 0 |
| 1 | 0 | 0 |
| 1 | 1 | 1 |

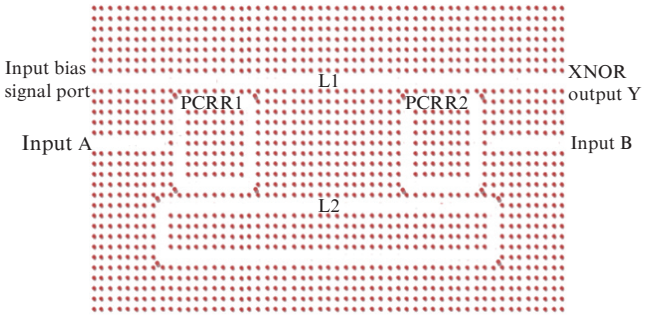


**Figure 3.** Overall structure of the optical XNOR gate based on a 2D square lattice of photonic crystals.

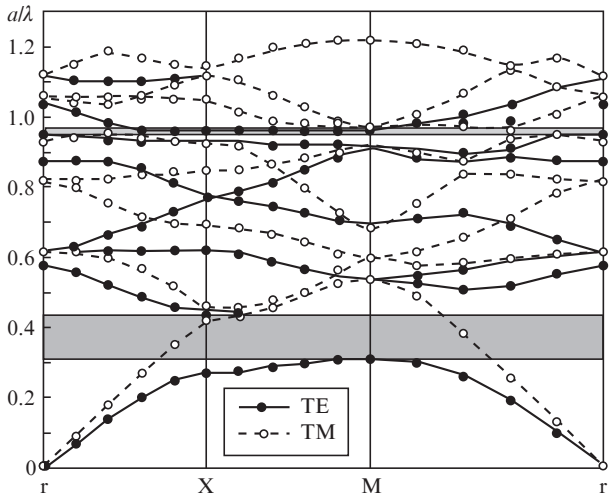


**Figure 4.** Bandgap structure diagram for photonic crystals with a square lattice of silicon rods of radius $0.21a$.

The plane wave expansion (PWE) [22] and finite difference time domain (FDTD) [23] methods are used to calculate the bandgap range of the overall structure. For the transverse electric TE mode, the normalised bandgap lies in the range $0.32 \leqslant a/\lambda \leqslant 0.44$, which, at a lattice constant $a$ = 630 nm, corresponds to the wavelength range 1432 nm < $\lambda$ < 1969 nm (Fig. 4). The key point of the photonic crystal is a structure with periodic variations in the dielectric constant. In the region of the photonic bandgap, light cannot propagate in the crystal structure and propagates only in the waveguide [21].

## 4. Simulation results of the optical XNOR gate

This section describes the optical XNOR performance and the results obtained for the proposed structure. The main idea of optical XNOR operation is based on the use of PCRRs, where the optical intensity is enhanced by triggering inputs A

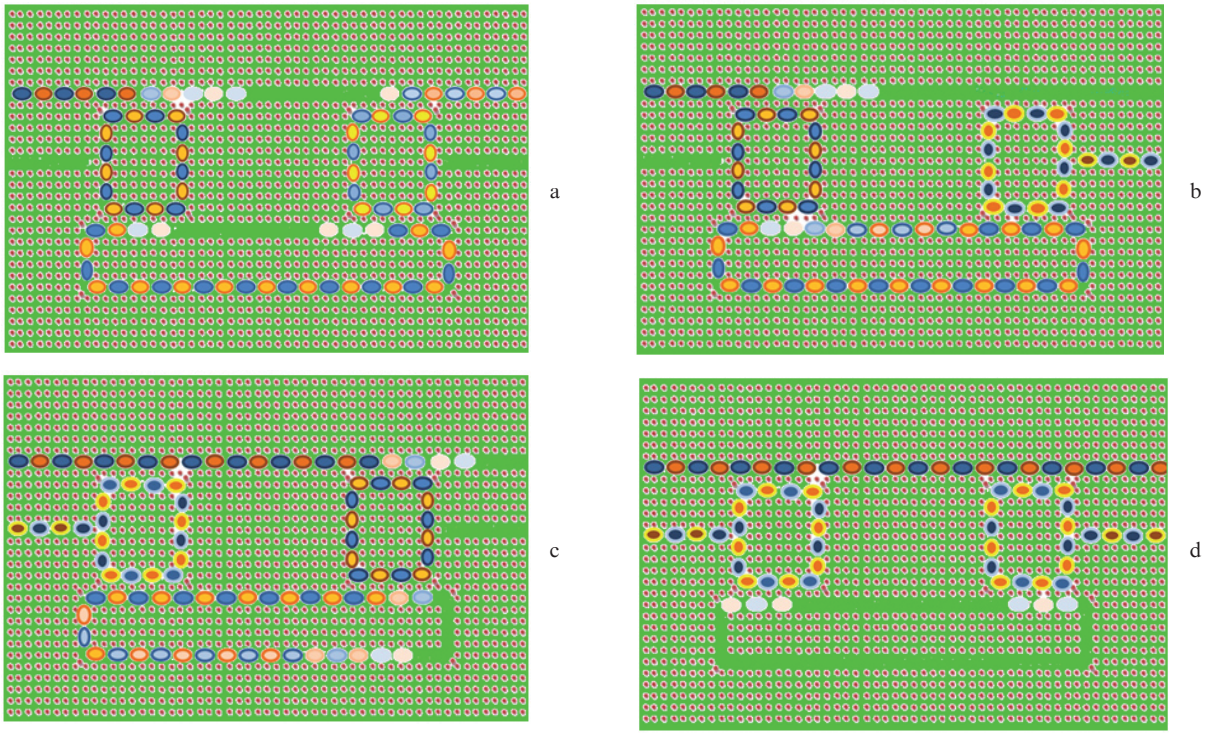


**Figure 5.** (Colour online) Electric field pattern of the optical XNOR gate for different inputs: (a) A = B = 0, (b) A = 0, B = 1, (c) A = 1, B = 0 and (d) A = B = 1.

and B to PCRRs. The optical bias signal power coupled to the input port through waveguide L1 is always logic high (1) (100 mW) at a wavelength $\lambda$ = 1550 nm. In addition, a sequence of optical logical inputs A, B is applied to the structure of the optical XNOR gate at a wavelength $\lambda$ =1560 nm to describe and realise the operation of the logic gate. Let us consider the following scenarios:

*Case 1*. At A = B = 0 (0 mW), the bias input optical field is dropped into PCRR1 by coupling to waveguide L2. The optical field which is coupled to waveguide L2 is directed to PCRR2 and dropped into this ring by coupling to waveguide L1 again. The optical signal coupled to waveguide L1 from PCRR2 is directed to the output port (Y) with an average optical power of the logical output (1) equal to 87 mW (Fig. 5a).

*Case 2*. At A = 0 (0 mW) and B = 1 (100 mW), the bias input optical field is dropped into PCRR1 by coupling to waveguide L2, and the optical signal of input B (100 mW) couples to PCRR2 to enhance the field intensity in ring resonator and prevents the coupling between waveguides L2 and L1 through PCRR2. Thus, the output of the XNOR gate Y is equal to logical zero (0) (Fig. 5b).

*Case 3*. At A = 1 (100 mW) and B = 0 (0 mW), the optical signal of input A (100 mW) couples to PCRR1 to enhance the field intensity in the ring resonator and prevents the coupling of the bias input to waveguides L1 and L2 through PCRR1 . The optical signal of the bias port is directed to PCRR2 and dropped into this ring resonator by coupling to waveguide L2, which gives output logical Y = 0 (14 mW) (Fig. 5c).

*Case 4*. At A = B = 1 (100 mW), the input optical bias signal flows directly to the output port Y = 1 (100 mW), where the signals of two input ports A and B are coupled to PCRR1 and PCRR2, respectively, and prevents the coupling of the optical bias input to waveguide L2 (Fig. 5d).

The optical NOT logic gate [4, 10, 13] would be used with the proposed XNOR structure at the output of the logic gate to implement the optical XOR gate, where the XOR gate is a logical complement of the XNOR gate.

Figure 6 shows the time dependent dynamics of the XNOR gate output at different inputs, where the experimental normalised output are simulated using FDTD and PWE methods. All the simulation results are scaled in arbitrary

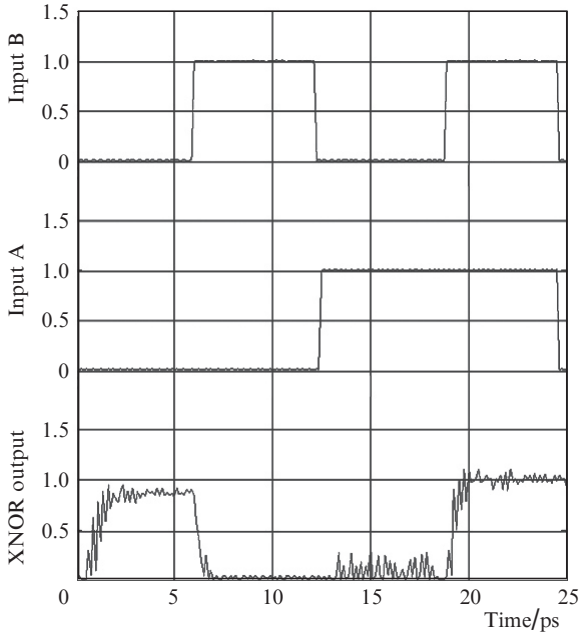


**Figure 6.** Results of simulation of the outputs for the proposed optical XNOR gate.

units at an input power of 100 mW. The transient rise time of the XNOR output is $t_r$ = 1.92 ps at A = B = 0 and 1.12 ps at A = B = 1 (Fig. 6), while the steady state time for the same cases of inputs is $t_{ss}$ = 2.96 and 1.73 ps, respectively.

Thus, the proposed structure of the XNOR gate can be used in modern communication networks to reach a very high rate and ultrafast data speed transfer.

## 5. Conclusions

The optical XNOR gate is an important logic gate, which can be useful in designing an optical half adder, full adder, logical comparator, network parity check and other combinational logic circuits based on photonic-crystal structures, where photonic crystals make them very promising for optical integrated circuits. Thus, the paper proposes a simple and novel optical XNOR based on two photonic-crystal ring resonators with a resonance wavelength equal to 1550 nm. The proposed optical XNOR structure can be converted to an optical XOR gate by using an optical NOT gate. The structure operation and efficiency are confirmed by analytical and numerical simulation of the proposed structure using FDTD and PWE methods.

## References


1. Ye Liu, Fei Qin, Zi-Ming Meng, Fei Zhou, Qing-He Mao, Zhi-Yuan Li. *Opt. Express*, **19** (3), 1945 (2011).
2. Wen-Piao Lin, Yu-Fang Hsu, Han-Lung Kuo. *Amer. J. Modern Phys.*, **2** (3), 144 (2013).
3. Yi-Pin Yang, I-Chen Yang, Chia Hsien Chang, Yao-Tsung Tsai, Kun-Yi Lee, Yi-Rung Tsai, Yong-Si Tu, Sin-Fu Liao, Ching-Chou Huang, Yen-Juei Lin, Wei-Yu Lee, Cheng-Che Lee. *Intern. Symp. on Computer, Consumer and Control* (Taichung, Taiwan, 2012).
4. Ghadrdan M., Mansouri-Birjandi M.A. *IJECE*, **3** (4), 478 (2013).
5. Tanabe T., Notomi M., Mitsugi S., Shinya A., Kuramochi E. *Appl. Phys. Lett.*, **87** (15), 151112 (2005).
6. Salmanpour A., Mohammadnejad S., Bahrami A. *J. Modern Optic*, **62** (9), 693 (2015).
7. Alipour-Banaei H., Mehdizadeh F., Serajmohammadi S. *Optik*, **124**, 5964 (2013).
8. Rostami A., Alipour Banei H., Nazari F., Bahrami A. *Optik*, **122**, 1481 (2011).
9. Ribeiro R.M., Lucarz F., Fracasso B. *Proc. 18th Europ. Conf. Network Opt. Commun. & Opt. Cabling Infrastructure* (NOC–OSI, 2013) (Graz, Austria, 2013) p. 35.
10. Moniem T.A. *J. Modern Optic*, **63** (8), 735 (2016).
11. Serajmohammadi S., Alipour-Banaei H., Mehdizadeh F. *Opt. Quantum Electron.*, **47** (5), 1109 (2015).
12. Alipour-Banaei H., Mehdizadeh F., Serajmohammadi S., Assangholizadeh-Kashtiban M. *J. Modern Optic*, **62** (6), 430 (2015).
13. Moniem T.A. *J. Modern Optic*, **62** (19), 1643 (2015).
14. Abbasi A., Noshad M., Ranjbar R., Reza K. *Opt. Commun.*, **285**, 5073 (2012).
15. Moniem T.A. *Opt. Quantum Electron.*, **47** (8), 2843 (2015).
16. Chin-Hui Chen, Shinji Matsuo, Kengo Nozaki, Akihiko Shinya, Tomonari Sato, Yoshihiro Kawaguchi, Hisashi Sumikura, Masaya Notomi. *Opt. Express*, **19** (4), 3387 (2011).
17. Serajmohammadi S., Absalan H. *Inform. Proces. Agriculture*, **3** (2), 119 (2016).
18. Mano M.M. *Computer Engineering: Hardware Design* (Englewood Cliffs, NJ: Prentice-Hall Intern., 1988).
19. Dang Z., Breese M., Recio-Sánchez G., Azimi S., Song J., Liang H., Banas A., Torres-Costa V., Martín-Palma R.J. *Nanoscale Res. Lett.*, **7**, 416 (2012).
20. Loncar M., Doll T., Vuckovic J., Scherer A. *J. Lightwave Technol.*, **18**, 1402 (2000).
21. Moniem T.A. *Opt. Quantum Electronics*, **48**, 424 (2016).
22. Johnson S.G., Joannopoulos J.D. *Opt. Express*, **8**, 173 (2001).
23. Gedney S.D. *Introduction to Finite-Difference Time-Domain (FDTD) Method for Electromagnetics* (Lexington, KY: Morgan and Claypool, 2010).